

1
2
3
4
5
6
7
8
9
10
11
12
13
14
15
16
17
18
19
20
21
22
23

DOI:

10.1002/arp.1529

Geophysical and Archaeological Characterization of a Modest Roman Villa: Methodological Considerations about Progressive Feedback Analyses in Sites with Low Geophysical Contrast

ÓSCAR PUEYO ANCHUELA^{1*}, PILAR DIARTE BLASCO², CARLOS GARCÍA BENITO³, ANTONIO M. CASAS SAINZ¹ AND ANDRÉS POCOVÍ JUAN¹

¹ Departamento de Ciencias de la Tierra, Universidad de Zaragoza, Zaragoza, Spain

² Escuela Española de Historia y Arqueología (EEHAR-CSIC), Rome, Italy

³ Departamento de Ciencias de la Antigüedad, Universidad de Zaragoza, Zaragoza, Spain

ABSTRACT

The low contrast in physical properties of archaeological elements compared to the host soil is a common drawback in geophysical surveys applied to subtle archaeological sites because those contrasts are usually what are being measured by most instruments. Furthermore, when archaeological elements and construction remains are placed within the same package of materials, differentiation of each can make the interpretation of geophysical data sometimes difficult. In This work we propose a dynamic, integrated approach for the characterization of an archaeological site with simple Roman construction materials in order to evaluate methodological considerations in the evaluation of this kind of sites. This approach includes: (i) a preliminary evaluation of construction material characteristics, according to the background provided by the historical and geographical context and from previous excavations, (ii) measurements of magnetic susceptibility of archaeological and natural materials in the site for

24 direct modelling of the expected anomalies; (iii) a geophysical survey including magnetometry,
25 multifrequency electromagnetic (EM) method and ground penetrating radar (GPR) (100, 250
26 and 500MHz centre frequency antennas); (iv) geophysical data evaluation for planning
27 subsequent systematic surveys; (v) dynamic interpretation of geophysical results through
28 careful data evaluation of all previous steps. The final archaeological model from geophysical
29 data has been successful due to the manner of data interpretation looking for orthogonal
30 patterns of geophysical anomalies that were hypothesized to be subsurface walls. Modelling
31 was then followed by archaeological excavations consisting of three trenches where the walls
32 were exposed. The integration of Geophysical data with excavations has permitted to evaluate
33 significance of the different geophysical analysis and to identify their archaeological meaning.
34 The proposed sequential methodology represents an innovative manner of analysis (i) in subtle
35 sites where construction remains are scarce and the absence of well-defined Geophysical
36 contrasts can limit the results of usual surveys and (ii) to increase the efficiency in the
37 evaluation of more extensive survey areas.

38 Key words: Roman villa; multidisciplinary approach; geophysical survey; Turiaso

39 **Introduction**

40 Geophysical analysis has been applied to identify and locate archaeological remains
41 and for the non-invasive characterization of archaeological sites. Geophysical techniques, with
42 different success to archaeology, have been widely applied including seismic, magnetic,
43 electric, electromagnetic (EM), gravimetric or ground penetrating radar (GPR) techniques,
44 among others [e.g. Belshe, 1957; Aitken, 1974; Hesse et al., 1986; Scollar, 1962; Linington,
45 1966; Bevan, 1983; Vaughan, 1986; the updated state of the art can be evaluated in Clark
46 (1996), Gaffney and Gater (2003) and Witten (2006) and references cited therein].

47 Approaches including more than one Geophysical technique are also common (Tsokas
48 et al., 1994; Neubauer and Eder-Hinterleitner, 1997; Batayneh et al., 2001; Pellerin, 2002;

49 Seren et al., 2004; Gaffney et al., 2004; Drahor, 2006, 2011; Drahor et al., 2008a; Forte and
50 Pipan, 2008; Bagaloni et al., 2011; Abbas et al., 2012; Apostolopoulos, 2014). The use of
51 Geophysical techniques in archaeology depends upon the site characteristics, time schedule,
52 budget and objectives. The optimal routine is the application of the maximum number of
53 techniques (in order to better characterize the site), with the highest possible resolution and
54 survey density. Some of these factors are not necessarily related to budget or time constraints
55 as the time needed to perform the geophysical survey is usually small compared to most
56 archaeological excavations. In this sense, Geophysical surveys are often used as a guide to
57 focus invasive analyses and to define the main target areas.

58 The application of any one particular Geophysical technique can be successful if the
59 contrasts of physical properties of the ground are well known, defined and do not vary
60 appreciably along the surveyed zone (e.g. Hesse, 1999; Ernenwein and Hargrave, 2009). In
61 cases where the targets are known but cannot be defined in terms of geophysical contrasts,
62 the selection of the optimal geophysical technique can be a difficult task. This subject can be
63 addressed considering the historical period and the construction style, but continuous re-
64 evaluation and adaptation of the Geophysical survey – including characteristics, processing and
65 interpretation manner – is recommended during the survey design and the geophysical work.

66 In this work, we present a geophysical survey carried out in a small Roman site (villa) in
67 Tarazona in northeast Spain (Figure 1). The study presented here applies a progressive
68 evaluation of the site characteristics through different research phases, including the selection
69 of geophysical techniques and interpretation manners depending upon the information
70 obtained during the previous phases. The objective was to characterize from a geophysical
71 point of view a site where surficial remnants and preliminary excavations suggested the
72 presence of the villa. The characteristics of the construction materials and the site

73 characteristics showed low geophysical contrasts owing to the low susceptibility contrasts with
74 respect to the host soil and the use of earth materials in the construction.

75 Therefore detailed processing and data interpretation were needed. Here we illustrate
76 the procedures applied for the geophysical characterization of this site that were subsequently
77 compared to excavations. We suggest that our approach that includes multiple sensors,
78 definition of targets and integration with excavations is important especially for Geophysical
79 surveys in contexts that have few substantial architectural remains with low contrasts
80 between the host soils and the archaeological elements.

81 **Historical and archaeological context**

82 The archaeological site of La Dehesa is located 10 km north of Tarazona (old Turiaso)
83 and 4km west of Cascante (old Cascantum), within the Ebro Basin of northeast Spain (Figure 1),
84 and belonging to the old Roman province of Hispania. The studied site is located at the top of a
85 small hill with bedrock consisting of subhorizontal or slightly sloping units of Cenozoic age
86 rocks composed of detrital deposits and evaporites (Zaragoza Fm., Miocene in age; Quirantes,
87 1978) (Figure 2a). In the northern portion of the site there are also anthropogenic deposits
88 (Figure 2b). It appears the area was inhabited from the Roman period to present, which
89 architecture composed of natural materials such as adobe, rammed earth or fired bricks.
90 Important cities nearby such as Caesaraugusta, Calagurris, Bilbilis, Pompaelo or Ilerda, used
91 opus caementicum, a type of roman concrete, for the construction of the main public and
92 private spaces (Figure 1).

93 However, in rural areas, such as our study site, construction was more commonly with
94 adobe or rammed earth bricks obtained from local sources, in contrast to the monumental and
95 usual buildings in cities, therein the low contrasts between architecture and the surrounding
96 matrix.

97 The test site is one of the first villae discovered for the archaeological research in the
98 central Ebro Basin. It was discovered in 1979, due to clandestine activities, without an
99 archaeological supervision, which showed numerous Roman remnants (Figure 2c). The site was
100 dated between the first and second century (Bona López et al., 1989; García Serrano, 2003;
101 Sanz Núñez, 1982). After the discovery in 1979, Centro de Estudios Turiasonenses (CET)
102 organized a collection of materials by conducting a small excavation with the participation and
103 assistance of the Provincial Museum of Zaragoza. Clandestine excavations, however, still
104 occurred during the 1980s. Professional activities were again initiated in 2012 when the CET
105 organized a surface survey following an intensive pattern, with straight lines covering the
106 whole area as an attempt to evaluate the areal distribution of the site and to protect its
107 extension that was within farming fields. On the surface, in addition to some of the identified
108 surficial archaeological remains, a structure 1.5m high defines a room excavated in 1979,
109 which is approximately 5m wide. Paving placed over an embankment at the north of the site
110 was also identified. Associated with this area Roman pottery remains, tiles, pieces of glass,
111 metal debris and decomposed remains of mortar and adobe were found.

112 The profusion of surface materials and their quality point to a significant centre of
113 activity of the Ager Turiasonense in a portion of the studied site. However, in spite of the
114 importance of this archaeological site that was likely associated with agricultural activities
115 during the early centuries of the roman High Empire (AD 70–192), it is probable that its main
116 buildings were still constructed with adobe or locally derived stone blocks. The amount and
117 wide distribution of surficial evidences related to ceramics and other elements at the surface
118 supported the hypothesis that a more extensive group of structures remained in the
119 subsurface, whose locations could not be determined from surface observation. Therefore,
120 only geophysical surveys could provide information about the buried structures and other
121 possible features. As the recovered archaeological remains suggested that this site is likely
122 non-monumental, it provided an excellent test for how geophysics, when carefully applied and

123 analysed could be used for the evaluation of sites from more everyday rural life in This area of
124 Spain during the Roman period.

125 **Site characterization, geophysical evaluation and targets definition**

126 The site characterization was performed through (i) an analysis of the historical-
127 archaeological site characteristics (historical, geological and field inspection of construction
128 remains dating of the same period), (ii) a preliminary evaluation in order to define the
129 subsequent geophysical survey (properties contrasts, techniques or needed data distribution),
130 (iii) survey following the interpretations obtained from the preliminary campaigns, (iv)
131 integrated evaluation and geophysical characterization of the archaeological structures in the
132 subsoil, (v) excavation of trenches considering the geophysical data and (vi) re-evaluation of
133 obtained data bearing in mind the results of the archaeological excavation.

134 **Phase 1. Analysis of data and archaeological-geophysical context**

135 Surficial data, accessible outcrops and clandestine excavations in the area permitted us
136 access to information for evaluating the physical characteristics of the site and to predict
137 geophysical contrasts that might produce anomalies in the geophysical surveys (Figure 2). The
138 stratigraphy in the area is composed of (i) near the surface a clay-rich surficial soil unit, ranging
139 in thickness from several centimetres in the northern part of the study area to 1.5m in the
140 southern zone, containing small roots, boulders, ceramic fragments and mosaic tiles and (ii)
141 underlain by a heterogeneous, grey-yellow unit containing archaeological building debris, coal
142 and ceramic remains (Figure 2d). The construction materials are composed of adobe, stones
143 and boulders. Walls can be defined by boulders, earth materials, concrete or mortar. In some
144 cases, a pavement between walls is composed of a compact earthen surface with additions of
145 mortar and ceramic fragments. Some of this information on the buried architecture was
146 obtained from previous excavations in the area located to the east of the study area (Figure

147 2e). Magnetic susceptibility of soils and architectural materials was easily measured in the
148 field with a hand-held susceptibility meter (KT-10, Terraplus).

149 Mean susceptibility values of various subsurface materials showed differences
150 between groups of materials, and a wide variety of materials from boulders to clay soils, with
151 compacted limes and multi-size particles of anthropogenic fill (Figure 3a). The highest
152 magnetic susceptibility values, which were several orders of magnitude higher than the other
153 analysed materials, were recorded in burned bricks and ceramic fragments. Their influence in
154 the magnetic survey was determined through forward modelling of theoretical magnetic
155 anomalies using susceptibility values measured in the field by 2.5D Gravmag software from the
156 British Geological Survey (Figure 3b). Obtained results indicate that ceramic elements,
157 depending on their depth, produce magnetic anomalies that can reach values between 1 and 3
158 nT. Boulders, that are usually part of construction elements, only produce significant
159 anomalies when they are close to the surface.

160 The highest value of magnetic anomalies, in the range of several tens of nanotesla,
161 were predicted to be ceramic and brick clusters near to the surface (Figure 3c). These forward
162 models also show that surficial elements not linked to archaeological remains can give similar
163 or even higher anomalies than the buried archaeological structures. The analysis of the
164 magnetic profiles obtained from the anomaly model permitted the identification of various
165 archaeological targets at different depths depending upon the amplitude and wavelength of
166 the magnetic anomalies. These results showed the potentially strong magnetic response of
167 surficial clusters of boulders and the loss of resolution when archaeological structures are
168 located below 1m depth.

169 **Phase 2. Preliminary geophysical campaign**

170 The theoretical predictions and an analysis of presumed buried archaeological targets
171 suggested a very low geophysical contrast in magnetic readings from the buried features.

172 However, magnetometry is a fast survey technique that can be used in order to locate areas to
173 initiate more detailed surveys when magnetic data show even low contrast measurements, as
174 distinct from more homogeneous results. Its effectiveness is noticeable especially where there
175 are concentrations of ceramic elements over and around buried structures, and can therefore
176 be used as an indirect indicator for the location of archaeological remnants. In this sense, and
177 due to the complexity in the evaluation of certain physical properties, a comparative analysis
178 of geophysical data between magnetic and other geophysical techniques was then carried out.
179 The objective of this analysis was to evaluate if there were a correlation between magnetic
180 anomalies that has been considered in the predictive models and other techniques that were
181 then tested in the study area.

182 The preliminary field surveys consisted of gathering data from each instrument along
183 the same transects using different geophysical devices (Figure 2e): (i) magnetometry [intensity
184 of the total magnetic field and vertical magnetic gradient; GSM-19, Overhauser magnetometer
185 having an incorporated global positioning system (GPS) and two sensors separated 0.5m as
186 rover, and a PMG1 proton precession magnetometer as a base]; (ii) electromagnetic
187 multifrequency survey (GEM-02; measurement of three different frequencies: 65, 18 and
188 5kHz]; (iii) GPR with shielded antennas of 100, 250 and 500MHz (Mala Geoscience, CUI-2). We
189 used the magnetic susceptibility data to evaluate and compare the results obtained from other
190 techniques because no data about the electromagnetic characteristics were available.
191 Magnetic profiles showed anomalies in the range of 4.6 and 6 nT and maximum vertical
192 magnetic gradients of 6 nT/m (Figure 4a). These values were within the expected range for
193 surficial construction elements obtained from the forward models (Figure 4a). EM data were
194 used for the calculation of apparent magnetic susceptibility and electrical conductivity values
195 (Huang and Won, 2000; Huang, 2005).

196 Apparent susceptibility shows mean values of 600×10^{-6} (SI units), similar to the values
197 obtained for soils and limes from direct magnetic susceptibility measurements, with slight
198 variations in the range of 50 to 100×10^{-6} (SI units), which occurred in the same general areas
199 where magnetic anomalies were identified. Apparent electrical conductivity shows progressive
200 changes for middle to high frequencies that represents shallow intervals (18 and 65kHz; Figure
201 4b). The highest amplitude variability and the lowest wavelength of anomalies are identified
202 for deeper ground intervals (5kHz). The anomalies size and the lateral correlation of them
203 through parallel profiles do not show clear map view distributions and they show a wider
204 scattering than susceptibility or magnetic anomalies. GPR profiles (Figure 5) show a general
205 shallow energy penetration, in the range of 1m, which was expected from the high apparent
206 surficial electric conductivity identified in the EM survey (between 100 and 150 mS/m; Figure
207 4b). There was no difference in energy penetration depths between the 100 and 250MHz
208 antennas due to this attenuation of energy at about 1m depth (Conyers, 2013). The Energy
209 penetration of 500MHz antenna was significantly lower, with energy reaching just a few
210 decimetres. Hyperbolic reflection features are better defined in the 500MHz profiles. In
211 general, reflection features visible in GPR profiles are coincident between profiles (Figure 5),
212 suggesting linear alignments in the ground.

213 The analysis of GPR profiles permitted the identification of buried features composed
214 of homogeneous materials, which varied in appearance depending on the antenna used. The
215 analysis of GPR profiles should present a homogeneous, parallel and horizontal banded
216 distribution of reflectors if underground is homogeneous. In this sense, an analysis of such
217 changes that modify the expected homogeneous underground structure was carried out. In
218 these analysis interruptions of the horizontal homogeneous underground structure identified
219 at 100MHz profiles, not horizontal reflectors at 100 and 250MHz and hyperbolic anomalies at
220 250 and 500MHz were considered. Changes in the definition of reflectors and their continuity

221 and reflectivity were considerable between parallel profiles, indicating the complex nature of
222 buried walls in the study area.

223 The previously described variations in the GPR profiles were then compared to
224 magnetic and EM data along coincident profiles. Magnetic anomalies are characterized by
225 dipoles and were mapped in the study area as positive or negative residuals. Both normal and
226 inverse dipoles generally coincide with the hyperbolic-shaped GPR reflections, and are
227 interpreted to be buried architectural features composed of slightly magnetic materials (Figure
228 5). These changes, subvertical interruptions of the underground structure, dipoles and
229 hyperbolic-shaped reflection features are distinct from areas where the ground is
230 homogeneous. In the case of EM data, anomalies show in general only small changes in
231 amplitude and longer wavelengths than the other techniques.

232 This comparison suggests a lower sensitivity and resolution of EM data compared to
233 the other techniques. The interpretation and evaluation of the preliminary campaign results
234 permitted us to establish some general guidelines for the subsequent systematic surveys.
235 These considerations pointed to the target definition, the survey distribution and the expected
236 resolutions that can be obtained depending upon the employed techniques and the obtained
237 results of anomalies sizes and contrasts. Since EM anomalies do not show the expected
238 pattern for archaeological remains, it was not used in the subsequent survey. However,
239 magnetic anomalies are small in size and in the expected range for the size of buried
240 archaeological remains. Moreover the identification of homogeneous magnetic domains (in
241 trend or in values) between alignments of anomalies recommended the use of magnetic
242 survey in the detailed campaign.

243 Magnetometry was therefore used for the overall survey as it provided a systematic
244 and fast characterization of the ground. These results then were used to define and focus on
245 areas for more detailed analysis by GPR. Each technique has different objectives: (i) magnetic

246 areal survey, in order to locate sectors where changes in the earth magnetic field were
247 identified and (ii) GPR survey with high density sampling following parallel profiles in two
248 normal directions in magnetically heterogeneous sectors. This approach was considered as it
249 allowed for the analysis of an extensive area and was then used to focus subsequent analysis
250 with GPR in selected zones.

251 **Magnetic areal survey.**

252 The magnetometry surveys covered 6000m² with 9000 measurement points collected
253 of intensity and vertical gradient taken along profiles having different orientations. At least,
254 one measurement point every square metre was collected. In advance of the survey, boulders
255 and the larger ceramics were picked up from the surface to avoid their potential influence to
256 the survey. The data was collected using a magnetometer with GPS that permitted the
257 locations of all readings. Magnetic data processing consisted of diurnal variation corrections,
258 filtering of data with low measurement definition and exclusion of anomalously high values
259 prior to data interpolation and gridding.

260 Magnetic anomalies in the raw data are on the range of 20 nT with the highest values
261 associated with surficial clusters of boulders and larger ceramic fragments, especially prevalent
262 in the northwest sector of the survey area. These clusters are likely related to previous farming
263 activities where these materials were removed from fields in recent times. Outside these
264 anomalously high magnetic sectors, the range of variation of the magnetic field is 10 nT and
265 anomalies usually do not exceed 2 nT. The vertical magnetic gradient map does not show
266 continuous anomalies, whereas the total magnetic field shows groups of anomalies with E-W
267 and NW-SE main orientations (Figure 6). This distribution of magnetic anomalies along linear
268 trends can be interpreted in terms of anthropic modifications of the underground subsoil
269 structure. The most significant change in the earth magnetic field survey is the identification of
270 a sector with higher magnetic field intensity (marked sector in Figure 6b) and alignments of

271 magnetic dipoles. This is the sector that was selected for GPR survey because it included not
272 expected natural magnetic anomalies alignments and sectors with higher intensity of magnetic
273 data laterally limited by dipoles alignments.

274 **GPR survey**

275 A 30m×20m grid was established in an area where several magnetic anomalies were
276 mapped (Figure 6b). Both 250 and 500MHz antennas were used with a grid of profiles in two
277 orthogonal directions. Profile separation was 1m with 80 total profiles. Traces were collected
278 at regular measurement intervals between 1 (500MHz) and 3 cm (250MHz) and defined by
279 1024 samples per trace. The survey was carried out with an odometer (survey wheel) attached
280 to the antennas.

281 Reflection processing consisted in zero time correction, amplitude gain (linear and
282 exponential), band-pass filtering for the removal of noise at both the high and low range of the
283 amplitude spectrums of each antenna, running averaging of traces to reduce random noise,
284 and background removal.

285 Data interpretation consisted of manual picking of areas where there were changes in
286 reflectivity, attenuation, clear reflectors, lateral interruption of reflectors and hyperbolic
287 anomalies. The identified reflections, which were mostly hyperbolic reflections from point
288 sources were then plotted to view their distribution. This map showed sectors with clusters of
289 hyperbolic reflections and also lateral interrupted planar reflections, all of these, suggests
290 buried walls and perhaps floors or cut and fill anthropogenic features. Changes between
291 reflective and attenuating media and the presence of hyperbolic reflections are suitable for
292 semi-quantitative analysis and amplitude maps were then constructed (Conyers, 2013). These
293 amplitude slicemaps permitted the identification of sectors with high reflectivity and also
294 zones of high density of hyperbolic reflections (Figure 7a). Amplitude slices were constructed
295 from 5 to 25ns depth (10 cm to 1.3m).

296 The mapped distribution of changes in reflectivity did not show an ordered distribution
297 of changes that was expected for archaeological buried structures. The comparison of these
298 GPR slice-maps (Figure 7a) show that higher reflective media and the visual identification of
299 concentrated hyperbolic-shaped point source reflections correlates with the middle to high
300 values of the magnetic field and the clustering of magnetic dipoles. There are still some
301 clusters of hyperbolic GPR reflections that coincide with low values of the magnetic field
302 (Figures 5 and 7b). This is interesting as it appears to show that the use of multiple sensors
303 here can not only identify the buried architecture but also identify its composition. The
304 forward models suggest that areas of adobe architecture will have low magnetic contrasts, but
305 will still generate GPR reflection hyperbolas.

306 Those composed of more magnetic materials such as burned bricks or boulders will
307 look similar in GPR profiles and amplitude maps, and also have a higher magnetic contrast.
308 When viewed in cross-section, these differences can be readily identified (Figures 8a and 8b).
309 These results permitted us to define, from a geophysical point of view, (i) areas where there
310 are changes of the structure of subsoil materials that have archaeological significance, and (ii)
311 homogeneous and heterogeneous areas that are more likely inter-feature areas.

312 **Interpretation and discussion**

313 **Construction of anomalies models with archaeological relevance**

314 Different geophysical approaches are usually employed for the characterization of
315 archaeological remains with different success. Magnetometry has shown a wide application in
316 archaeology, especially for the identification of archaeological elements with high
317 susceptibility contrasts, usually related to artificial, buried objects, burnt features and rubbish
318 deposits. Magnetic anomalies in archaeological sites usually exceed in amplitude the
319 anomalies identified in this work and they are related to artificial elements in graves (10–20
320 nT; e.g. Özgü Arısoy et al., 2007), bricks and metal deposits within the archaeological

321 structures (Drahor et al., 2008b), burnt features and rubbish deposits (10–15 nT; Gaffney and
322 Gater, 2003), pottery kilns (Tsokas and Hansen; 2000), pithouses (reaching 50 and over 1000
323 nT, Eppelbaum et al., 2010; Rogers et al., 2011; Argote et al., 2000), storage pits (e.g. Rego and
324 Cegielski, 2014; with anomalies between 10 and 14 nT) or monumental structures of large
325 scale (e.g. Caggiani et al., 2012; with more than 50 nT of variation range).

326 In general, the distribution of magnetic anomalies in map view does not define a three-
327 dimensional (3D) construction pattern except when these anomalies are linked to monuments,
328 present a well defined susceptibility contrast with respect to the host soil or when there are no
329 construction elements dispersed around constructions. In many cases, anomalies related to
330 buried buildings are determined by the clustering of high susceptibility elements that are
331 contained within, or surrounding, archaeological structures. When adobe structures or local
332 natural materials are used for construction, as the presented case, they define subtle
333 anomalies that can be difficult to isolate from the host soil. Moreover, the presence of
334 collapsed walls and buildings and the subsequent farming activity can significantly challenge
335 the interpretation and data processing in this kind of site. For this case, long-wavelength
336 anomalies and zones where magnetic anomalies cluster can be used as an indirect indicator of
337 heterogeneous, non-natural domains.

338 The use of resistivity or EM methods, excluding GPR, has also permitted the
339 characterization of archaeological features but, in general, with long wavelengths or low
340 resolution results. These data have been used for the location of non-natural subsoil
341 structures, the evaluation of areas suitable for applying other Geophysical techniques or direct
342 excavation. In some cases wide anomalies have been identified over archaeological buried
343 structures (Witten et al., 2000; Urban et al., 2014) or decametric structures (Drahor et al.,
344 2008a; De Smedt et al., 2013, 2014; Zheng et al., 2013). In these works similar conclusions to

345 the presented EM survey were obtained, reducing its applicability due to resolution
346 requirements and the particular site characteristics.

347 In the case of GPR, clear ordered patterns of reflectivity anomalies have been obtained
348 in cases where archaeological structures are located within a homogeneous soil or where
349 there are no collapsed structures or boulders disseminated between the archaeological
350 structures (e.g. Conyers, 2004, 2012, 2013). In other cases, changes in the reflectivity or
351 clusters of anomalies have been used in order to define monumental structures (e.g.
352 Papadopoulos et al., 2002), or, at an intermediate scale, the potential presence of
353 archaeological features can be detected through amplitude grid maps (e.g. Lasaponara et al.,
354 2014). With Independence of these aspects, even in cases of adobe constructions, GPR
355 anomalies are expected (e.g. Sternberg and McGill, 1995). Integrated geophysical multi-
356 technique analysis has been employed to achieve more robust interpretations or to determine
357 the origin of anomalies by feedback analysis.

358 The analysis of previous works in this subject shows that results are, in many cases,
359 site-dependent. Different correlations have been proposed between the results of geophysical
360 techniques and archaeological structures, showing (i) wide EM anomalies, but not significant
361 magnetic or GPR anomalies (Witten et al., 2003) over construction elements, (ii) electrical
362 resistivity tomography (ERT) anomalies related to walls and high overprint on these structures
363 of high susceptibility elements in the magnetic data (Drahor et al., 2008a) or (iii) GPR and
364 magnetic data correlations without clear patterns in map view distribution (Lasaponara et al.,
365 2014). With independence of these limitations, for certain cases where techniques and the
366 terrain characteristics are suitable, some considerations about the urban construction style
367 and map view distribution can be found integrating different techniques (e.g. Shaaban and
368 Shaaban, 2001; with ERT and GPR).

369 In the presented case, although there are not clear patterns of distribution of
370 geophysical anomalies, a direct correlation between the different geophysical results has been
371 obtained. This correlation reveals that GPR and magnetometry are sensitive to changes in the
372 subsoil structure, although anomalies cannot be univocally related to archaeological building
373 remains.

374 In order to decipher the origin of these anomalies and their potential correlation with
375 archaeological structures, some methodological considerations were established, following the
376 available archaeological and historical information: (i) the identified anomalies are associated
377 with objects that are included within the soil and can be related to structures, either in situ or
378 displaced from their original position; (ii) the identification of homogeneous trends in
379 magnetic anomalies or reflective sectors at the GPR can be related to pavements or
380 anthropogenic levels; (iii) the clustering of anomalies reveals the proximity to structures, not
381 necessarily in situ; (iv) at least three anomalies located along a straight line can be used as an
382 indicator of a linear structure (two of them located in two adjacent profiles). These rules were
383 used for data reinterpretation and the construction of an archaeological model for geophysical
384 data. In a first step, at the coincident area surveyed by magnetics and GPR, homogeneous and
385 heterogeneous domains in the subsoil were mapped.

386 This analysis consisted in the correlation between sectors having reflective or
387 attenuated media in the GPR and where magnetic field and vertical gradient show
388 homogeneous trends. This analysis was done defining sectors for each technique and analysing
389 their overlapping. The limits between these domains were established by the behaviour
390 change and, in some cases, following alignments of hyperbolic anomalies or magnetic dipoles.
391 This approach excludes elements that produce isolated anomalies without direct correlation
392 between parallel profiles. An example of step-by-step procedure is included in Figure 9. In

393 Figure 9a the distribution of anomalies identified at GPR (mainly hyperbolic anomalies but also
394 the lateral distribution of reflective media in the subsoil) has been included.

395 In this plot GPR anomalies are distributed along the study area without a clear
396 pattern. If magnetic anomalies are considered along a selected profile (Figure 9b) a correlation
397 with GPR hyperbolic anomalies is identified. This correlation was also evident in the
398 preliminary survey. From a conceptual point of view, walls can be interpreted in cases where
399 correlation of hyperbolic anomalies along GPR profiles is possible and only when they show a
400 parallel distribution in magnetic susceptibility changes. The integrated analysis permitted to
401 separate homogeneous and heterogeneous domains in terms of GPR and magnetic data. This
402 evaluation permits to exclude anomalies that can be related to isolated blocks or clusters of
403 blocks around collapsed buildings, or resulting from farming activities. Therefore, some
404 anomalies can be interpreted in terms of walls or archaeological remnants (Figure 9c) against
405 other anomalies that show a geophysical record not consistent with in situ archaeological
406 structures. A more detailed sketch of the evaluated factors to distinguish archaeological
407 structures in each of the identified anomalies and their correlation is included in Figure 9d.

408 The map distribution of anomalies (magnetic survey) or amplitudes (GPR) did not
409 permit to identify a clear pattern of archaeological structures. However, the profile evaluation
410 permitted to identify homogeneous magnetic domains laterally delimited by alignment of
411 anomalies (dipoles or hyperbolas). This evaluation permitted to exclude anomalies from the
412 studied zone that do not have a direct correlation to structures and the distribution of
413 anomalies following the described approach showed along the studied zone an ordered
414 distribution. Interpretation following a visual inspection of homogeneous and heterogeneous
415 domains, and later the evaluation of lateral correlation of anomalies has permitted to interpret
416 the anthropogenic, archaeological underground structure. In the case of the GPR, buried
417 structures have only been interpreted when a straight correlation between, at least, three

418 anomalies in three different parallel profiles were found. Homogeneous magnetic domains or
419 sectors with homogeneous attenuating or reflective media in GPR profiles and delimited by
420 linear structures, were interpreted as spaces between archaeological structures. In this model,
421 anomalies that do not follow the previously defined rules were not considered in the
422 construction of the geophysical model. This model permitted to identify an ordered pattern of
423 anomalies with the expected geometry for buried archaeological structures (Figure 9b).

424 **Analysis of the significance of the model of anomalies**

425 The proposed model of correlation of anomalies can be interpreted in terms of
426 archaeological structures and pavements between them. This approach permitted the
427 identification of ordered patterns of elements that were not identified or were difficult to
428 analyse from a direct data analysis without a manual, detailed interpretation. However, this
429 kind of analysis, which conceptually can be of application and can be successful, cannot be
430 validated without comparison with direct excavations. During 2012, a partial archaeological
431 excavation campaign was carried out along representative domains of the geophysical model
432 and also exceeding the anomaly distribution to define if the homogeneous trends between
433 anomalies could be related to natural soils or areas without clear archaeological structures.
434 Three trenches were dug in order to characterize sectors where alignments of anomalies
435 intersect (Figures 10a and 10b). In the three excavations construction remains were found.
436 These remains are two cistern with probable industrial use and a third one, whose utility could
437 not be defined. It was surprising to find these industrial remains in a sector where structures
438 for domestic use were previously found (block found in 1979, remains of a large pavement to
439 the north of the archaeological site and domestic potteries).

440 All in all, the correlation between the geophysical results and the archaeological
441 remains was confirmed (Figure 10c). In trench C (Figure 10d) a group of decimetric walls
442 composed of natural boulders with mortar and tessellae was found. The space between walls,

443 that has not a clear functional attribution, presents a heterogeneous structure with
444 construction elements, adobe bricks and mortar fragments. The geophysical model for this
445 sector showed small hyperbolic anomalies with reflective media and a heterogeneous sector
446 between the alignments of hyperbolic anomalies. This can be interpreted as the filling of the
447 space between walls by inward collapse. Magnetic susceptibility of analysed materials shows
448 low to intermediate values of susceptibility, similar to that identified for boulders and soils,
449 with heterogeneous values for the mortar levels. The intensity of magnetic field for this area
450 showed intermediate to high values, especially in correlation to hyperbolic anomalies and
451 reflective media. Trench D (Figure 10e) was located in a well defined alignment of small
452 anomalies within a heterogeneous domain. The space between these alignments presented
453 homogeneous vertical magnetic gradient values and low intensity of magnetic field. The
454 excavation showed three walls forming a U-shaped structure, composed of different
455 construction styles and made of concrete, mortar as cement, rocks and ceramic fragments.
456 Between the walls, a pavement and a high concentration of boulders, adobe bricks and mortar
457 fragments were identified. The pavement is composed of mortar, sand and small rock
458 fragments. In contrast with the previously described trench, the Geophysical model did not
459 permit to isolate the different walls identified in the trenches. This sector showed a
460 homogeneous signature in magnetometry and a heterogeneous GPR-domain limited laterally
461 by alignments of anomalies.

462 Geophysical data did not permit to identify the exact origin of the different isolated
463 elements, and it was considered as related to an anthropic structure. Excavation of this
464 element showed a small industrial pool defined by construction walls and an anthropic
465 pavement between them. Two orthogonal walls were identified in trench E (Figure 10f), which
466 can be interpreted as part of a pool for industrial purposes of hydraulic character. The
467 construction characteristics for walls and soil are similar to trench D. Geophysical data
468 permitted to identify a wide archaeological structure confirmed as walls with two normal

469 directions and a pavement between them. As in the case of trench D, the susceptibility
470 measurements in the excavation show middle to low values, in the range of the measured
471 soils. Mortar showed slightly lower susceptibility values but within a very variable range.
472 Magnetic data show small dipoles of magnetic vertical gradient at the limits of the structure,
473 homogeneous trends between them, and lower values for the total magnetic field for the
474 inner area with respect to its surroundings. The geometry of the archaeological remains was
475 drawn from the geophysical model, although the marginal walls were not clearly defined as
476 isolated structures.

477 Considerations about the applied methodology As previously stated, geophysics has
478 been usually employed in archaeological characterization and it represents invaluable
479 information for subsequent archaeological excavation. However, local archaeological
480 characteristics and construction style can limit the potential Geophysical results or make
481 difficult their interpretation. The use of adobe structures and local rocks for urban
482 construction is common in the Central Ebro Basin but also in buildings that do not represent a
483 monumental development or do not have social or cultural uses. The comprehension and
484 research of this kind of structures can be of higher interest than monumental structures
485 because they are more sensitive and representative of the life style. However, this kind of
486 interesting research subjects present identification problems both for traditional
487 archaeological and geophysical research. In this work, an approach that can be of wide interest
488 and applicability in this kind of complex contexts has been carried out. In the analysed case,
489 low relevance constructions, scarce remains and low geophysical contrasts define the
490 archaeological site. Traditional manners of interpretation of anomalies has not permitted the
491 site characterization due to the presence of elements with similar or higher geophysical
492 contrast than those related to the buried archaeological structures. The proposed approach
493 through the definition of some rules has permitted to define a walkthrough interpretation of
494 anomalies with archaeological relevance. The proposed routine has been applied following a

495 progressive definition of targets, objectives, contrasts, techniques and methodologies (Figure
496 11) that are shared in many research projects.

497 The different research phases can be grouped into a ‘preliminary phase’ when the site
498 can be evaluated from local or regional information. This first phase permits to constrain the
499 methodologies or approaches to be applied. The second phase includes the ‘site analysis and
500 survey design’ considering (i) geophysical noises, (ii) extension of the site, and (iii) surficial
501 analysis to evaluate the expected contrasts of properties between archaeological features and
502 the natural terrain. These data can permit to delineate a first geophysical campaign where
503 resolution, discrimination availability, amplitude and wavelength of anomalies for different
504 techniques can be evaluated. This evaluation should permit the geophysical design in terms of
505 resolution and data density.

506 However, usual processing and presentation procedures did not permit to identify the
507 archaeological remains in the subsoil. In this case, we propose a ‘more detailed data
508 interpretation’ stage, following the discrimination of sectors with high density of anomalies
509 that can be related to archaeological structures themselves or to the urban design. In this
510 phase, manual separation of in situ archaeological elements and displaced or natural elements
511 was based on their lateral correlation in parallel profiles. After this evaluation, a map view or
512 anomalies model distribution can be double checked with excavation. This comparison is the
513 stage of ‘feedback evaluation with the previous geophysical model’, aimed at modifying or
514 validating the geophysical interpretation. The limited contrasts between host rock and buried
515 archaeological remains and the distribution of debris are usually a threshold for geophysics in
516 this kind of site.

517 Magnetic anomalies do not allow unequivocal interpretations because of the low
518 contrasts between natural materials and archaeological remains, the different signature of
519 archaeological features (with both low and high susceptibilities), the strong imprint of ceramic

520 elements in magnetic data and the presence of construction elements without direct
521 connection with structures. These factors have limited the preliminary direct reconstruction of
522 the archaeological structure from magnetic data, map distribution of hyperbolic anomalies or
523 amplitude grid maps. Therefore, a detailed analysis is necessary to differentiate between in
524 situ and displaced archaeological remains and to identify ordered anomaly patterns with
525 independence of their geophysical signature. In this sense, data reinterpretation in terms of
526 lateral continuity of anomalies, with independence of their signature, is a correct approach in
527 order to delineate the buried structure of the archaeological site.

528 **Conclusions**

529 The integrated analysis of La Dehesa site in Tarazona (northeast Spain), including
530 geophysical analysis in different steps, and excavation, has permitted to evaluate the success
531 of integrated analysis at a roman villa. These archaeological sites do not contain significant
532 architectural elements and the construction materials do not present properties significantly
533 different with respect to the natural materials. Our analysis has considered a preliminary
534 target definition where small contrasts between archaeological remains and the host soil have
535 been identified. Different Geophysical signatures depending upon the construction materials
536 (adobe bricks, stone blocks and mortars) produced both positive and negative magnetic
537 anomalies. The distribution of these elements both in situ and displaced from their original
538 position and the dispersión at the surface of high susceptibility elements (ceramics) precluded
539 the identification of an ordered pattern of anomalies at a preliminary interpretation stage.

540 GPR and magnetic techniques show congruent results, although they do not permit to
541 obtain a simple or direct picture of the archaeological features. Nevertheless, feedback
542 analysis and continuous re-evaluation of geophysical data and comparison with previous and
543 new excavations, has permitted to adapt the Investigation to the local characteristics of the

544 site. Moreover, detailed analysis and lateral correlation of anomalies have shown the potential
545 application of the presented methodological approach for this kind of archaeological site.

546 The analysis, interpretation and survey routine presented can be of interest for the
547 characterization of archaeological sites that do not include monumental architectures but can
548 be more representative of the actual life of inhabitants.

549 **Acknowledgements**

550 This research has been financed by the Aragón Government (Geotransfer research group) and
551 Centro de Estudios Turiasonenses (Fernando el Católico Institution, Zaragoza). The authors
552 want to acknowledge comments, suggestions and advice from Larry Conyers and Chris Gaffney
553 as editors and two anonymous reviewers.

554 **References**

555 Abbas AM, Khalil M, Massoud U, et al. 2012. The implementation of multi-task geophysical
556 survey to locate Cleopatra Tomb at Tap-Osiris Magna, Borg El-Arab, Alexandria, Egypt 'Phase
557 II'. NRIAG Journal of Astronomy and Geophysics 1: 1–11. Aitken M. 1974. Physics and
558 Archaeology, 2nd edn. Clarendon Press: Oxford.

559 Apostolopoulos G. 2014. Combined geophysical investigation for the detection of ancient
560 metallurgical installations near Keratea City, Greece. Journal of Applied Geophysics 104: 17–
561 25.

562 Argote DL, Tejero A, Chávez RE, López PA, Bravo R. 2000. 3D modelling of magnetic data from
563 an archaeological site in north-western Tlaxcala state, Mexico. Journal of Archaeological
564 Science 36: 1661–1671.

565 Bagaloni V, Perdomo S, Ainchil J. 2011. Geoelectric and magnetic surveys at La Libertad
566 archaeological site (San Cayetano County, Buenos Aires Province, Argentina): a
567 transdisciplinary approach. *Quaternary International* 245: 13–24.

568 Batayneh A, Al-Zoubi A, Tobasi U, Haddadin G. 2001. Evaluation of archaeological site potential
569 on the Tall al-Kharrar area (Jordan) using magnetic and electrical resistivity methods.
570 *Environmental Geology* 41: 54–61.

571 Belshe J. 1957. Recent magnetic investigations at Cambridge University. *Advances in Physics* 6:
572 192–193. Bevan B. 1983. Electromagnetics for mapping buried earth features. *Journal of Field*
573 *Archaeology* 10: 47–54.

574 Bona López IJ, Albuixech AI, Núñez Marcén J. 1989. 'La Dehesa (Tarazona'. In *El Moncayo. Diez*
575 *años de investigación arqueológica y prólogo de una labor de futuro*, Bona López IJ et al. (eds).
576 *Centro de Estudios Turiasonenses: Tarazona*; 117–118.

577 Caggiani M, Cimnale M, Gallo D, Noviello M, Salvemini F. 2012. Online non destructive
578 archaeology: the archaeological park of Egnazia (southern Italy) study case. *Journal of*
579 *Archaeological Science* 39: 67–75.

580 Clark AJ. 1996. *Seeing Beneath the Soil. Prospecting Methods in Archaeology*. B.T. Batsford Ltd:
581 London.

582 Conyers LB. 2004. *Ground-penetrating Radar for Archaeology*. Alta Mira Press: Walnut Creek,
583 CA; 203 pp.

584 Conyers LB. 2012. *Interpreting Ground-penetrating Radar for Archaeology*. Left Coast Press:
585 Walnut Creek, CA.

586 Conyers LB. 2013. *Ground-penetrating Radar for Archaeology*. Alta Mira Press: Walnut Creek,
587 CA; 258 pp.

588 De Smedt P, Saey T, Lehouck A, et al. 2013. Exploring the potential of multi-receiver EMI survey
589 for geoarchaeological prospection: a 90 ha dataset. *Geoderma* 199: 30–36.

590 De Smedt P, Van Meirvenne M, Saey T, Baldwin E, Gaffney C, Gaffney C. 2014. Unravelling the
591 prehistoric landscape at Stonehenge through multi-receiver EMI. *Journal of Archaeological*
592 *Sciences* 50: 16–23.

593 Drahor MG. 2006. Integrated geophysical studies in the upper part of Sardis archaeological
594 site, Turkey. *Journal of Applied Geophysics* 59: 205–223.

595 Drahor MG. 2011. A review of integrated geophysical investigations from archaeological and
596 cultural sites under encroaching urbanisation in Izmir, Turkey. *Physics and Chemistry of the*
597 *Earth* 36: 1294–1309.

598 Drahor MG, Berge MA, Kurtulmus TÖ, Hartmann M, Speidel MA. 2008a. Magnetic and
599 electrical resistivity tomography. Investigations in a Roman legionary camp site (Legio IV
600 Scythica) in Zeugma, southeastern Anatolia, Turkey. *Archaeological Prospection* 15: 159–186.

601 Drahor MG, Kurtulmus TÖ, Berge MA, Hartmann M, Speidel MA. 2008b. Magnetic imaging and
602 electrical resistivity tomography studies in a Roman Military installation found in Satala
603 archaeological site from northeastern of Anatolia, Turkey. *Journal of Archaeological Science*
604 35: 259–271.

605 Eppelbaum LV, Khesin BE, Itkis SE. 2010. Archaeological geophysics in arid environments:
606 examples from Israel. *Journal of Arid Environments* 74: 849–860.

607 Ernenwein E, Hargrave M. 2009. *Archaeological Geophysics for DoD Field Use: a Guide for New*
608 *and Novice Users, Report*. US Army Corps of Engineers: Washington, DC; 109 pp.

609 Forte E, Pipan M. 2008. Integrated seismic tomography and ground-penetrating radar (GPR)
610 for the high resolution study of burial mounds (tumuli). *Journal of Archaeological Science* 35:
611 2614–2623.

612 Gaffney C, Gater J. 2003. *Revealing the Buried Past: Geophysics for Archaeologists*. Tempus
613 Publishing: Stroud.

614 Gaffney V, Patterson H, Piro S, Goodman D, Nishimura Y. 2004. Multimethodological approach
615 to study and characterize Forum Novum (Vescovio, Central Italy). *Archaeological Prospection*
616 11: 201–212.

617 García Serrano JA. 2003. *Arqueología del Moncayo*. Catálogo de la exposición permanente.
618 Centro de Estudios Turiasonenses: Tarazona; 122–123: 150–151.

619 Hesse A. 1999. Multi-parametric survey for archaeology: how and why, or how and why not?
620 *Journal of Applied Geophysics* 41: 157–168.

621 Hesse A, Jolivet A, Tabbagh A. 1986. New prospects in shallow depth electrical surveying for
622 archaeological and pedological applications. *Geophysics* 51: 585–594.

623 Huang H. 2005. Depth of investigation for small broadband electromagnetic sensors.
624 *Geophysics* 70(6): G135–G142.

625 Huang H, Won JJ. 2000. Conductivity and susceptibility mapping using broadband
626 electromagnetic sensors. *Journal of Environmental and Engineering Geophysics* 5: 31–41.

627 Lasaponara R, Luecci G, Masini N, Persico R. 2014. Investigating archaeological looting using
628 satellite images and georadar: the experience in Lambayaque in north Peru. *Journal of*
629 *Archaeological Science* 42: 216–230.

630 Linington R. 1966. Test use of a gravimeter on Etruscan chamber tombs at Cerveteri.
631 *Prospezioni Archeologiche* 1: 37–41.

632 Neubauer W, Eder-Hinterleitner A. 1997. Resistivity and magnetics of the Roman town
633 Carnuntum, Austria: an example of combined interpretation of prospection data.
634 *Archaeological Prospection* 4: 179–189.

635 Özgü Arısoy M, Özdemir K, Büyüksaraç A, Bilim F. 2007. Images of buried graves in Bayat,
636 Afyon (Turkey) from high-resolution magnetic data and their comparison with preliminary
637 excavations. *Journal of Archaeological Science* 34(1): 1473–1484.

638 Papadopoulos NG, Sarris A, Salvi MC, Dederix S, Soupios P, Dikmen U. 2002. Rediscovering the
639 small theatre and amphitheatre of ancient Ierapytna (SE Crete) by integrated geophysical
640 methods. *Journal of Archaeological Science* 39: 1960–1973.

641 Pellerin L. 2002. Application of electrical and electromagnetic methods for environmental and
642 geotechnical investigations. *Surveys in Geophysics* 23: 101–132.

643 Quirantes J. 1978. Estudio sedimentológico y estratigráfico del Terciario Continental de Los
644 Monegros. *Publicación Institución Fernando el Católico: Zaragoza*; 208.

645 Rego HP, Cegielski WH. 2014. Gradiometry survey and magnetic anomaly testing of Castros de
646 Neixón, Galicia, Spain. *Journal of Archaeological Science* 46: 417–427.

647 Rogers MB, Faehndrich K, Roth B, Shear G. 2011. Cesium magnetometer surveys at a Pithouse
648 Site near Silver City, New Mexico. *Journal of Archaeological Science* 37: 1102–1109.

649 Sanz Núñez AC. 1982. Métodos geofísicos aplicados a la prospección arqueológica. *Tvriaso III*:
650 9–27: .

651 Scollar I. 1962. Electromagnetic prospecting methods in archaeology. *Archaeometry* 5: 146–
652 153.

653 Seren S, Eder-Hinterleitner A, Neubauer W, Groh S. 2004. Combined high resolution magnetics
654 and GPR surveys of the Roman town of Flavia Solva. *Near Surface Geophysics* 2: 63–68.

655 Shaaban FF, Shaaban FA. 2001. Use of two-dimensional electric resistivity and ground
656 penetrating radar for archaeological prospecting of the ancient capital of Egypt. *African Earth*
657 *Sciences* 33: 661–671.

658 Sternberg K, McGill JW. 1995. Archaeology studies in southern Arizona using ground
659 penetrating radar. *Journal of Applied Geophysics* 33: 209–225.

660 Tsokas GN, Giannopoulos A, Tsourlos P, et al. 1994. A large scale geophysical survey in the
661 archaeological site of Europos (N. Greece). *Journal of Applied Geophysics* 32: 85–98.

662 Tsokas GN, Hansen RO. 2000. On the use of complex attributes and the inferred source
663 parameter estimates in the exploration of archaeological sites. *Archaeological Prospection* 7:
664 17–30.

665 Urban TM, Rowan YM, Kersel MM. 2014. Groundpenetrating radar investigations at Marj
666 Rabba, a Chalcolithic site in the lower Galilee of Israel. *Journal of Archaeological Science* 46:
667 96–106.

668 Vaughan CJ. 1986. Ground penetrating radar surveys used in archaeological investigations.
669 *Geophysics* 51: 595–604.

670 Witten A. 2006. *Handbook of Geophysics and Archaeology*. Equinox Publishing Ltd: London.

671 Witten A, Calvert G, Witten B, Levy T. 2003. Magnetic and electromagnetic induction studies at
672 archaeological sites in southwestern Jordan. *IEEG* 8: 209–215.

673 Witten AJ, Levy TE, Adams RB, Won LJ. 2000. Geophysical surveys in the Jebel Hamrat Fidan,
674 Jordan. *Geoarchaeology* 15(2): 135–150.

675 Zheng W, Li X, Lam N, et al. 2013. Applications of integrated geophysical method in
676 archaeological surveys of the ancient Shu ruins. *Journal of Archaeological Science* 40: 166–175.

677 Figure Captions

678 Figure 1. Geographical location of the studied zone with the main roman cities in the Iberian
679 peninsula. The inset shows the location of Turiaso and the analyzed site.

680 Figure 2. (a) General view of the studied zone and detailed photographs of surficial
681 archaeological remains: (b) archaeological remains along its northern limit; (c) exposed
682 remains in a previous excavation in the site; (d) cluster of boulders with stone blocks and
683 ceramic elements; and (e) aerial photograph from the studied site with the location of the
684 preliminary and detailed studied zone; clandestine trenches are also marked.

685 Figure 3. (a) Magnetic susceptibility values measured in the analyzed site. Inset shows the
686 table of mean susceptibility values and their standard deviation. (b) Model of anomalies
687 attending different elements related to high susceptibility contrast at different depths or
688 isolated boulders at the surface. (c) Complex magnetic anomalies model considering
689 archaeological construction remains at intermediate depths and analysis of the influence of
690 boulders and archaeological elements at subsuperficial conditions. Mean susceptibility values
691 of elements and background are included in the figure. The size of modeled elements has been
692 increased to help readability; actual size is included in the plots.

693 Figure 4. Results from the preliminary campaign along the same profile for magnetic and EM
694 surveys (a) magnetic data (intensity of Earth's magnetic field and vertical gradient) and
695 apparent magnetic susceptibility values from GEM-02 device for the 5 KHz frequency. (b)
696 Apparent conductivity sections for different frequencies.

697 Figure 5. Comparison of magnetic field data and the GPR profiles for 100, 250 and 500 MHz.
698 The main changes identified in the GPR profiles are highlighted.

699 Figure 6. (a) Areal survey for vertical magnetic gradient and magnetic field along the surveyed
700 area. (b) Presentation in false relief of data obtained from intensity of magnetic field and area
701 delimited by alignments of anomalies

702 Figure 7. (a) Apparent reflectivity maps for GPR data with different interpolation distances. The
703 TWT selected interval represents the equivalent to 1 m depth and the TWT interval for deeper
704 conditions than the location of anomalies (over 1.5 m). (b) Cartography of hyperbolic
705 anomalies and superposition on magnetic data. In both figures the profiles analyzed in Figure 8
706 are marked.

707 Figure 8. Example of comparative analysis along two selected transects whose location is
708 shown in Figure 7b. (a) Earth's magnetic field and vertical gradient anomalies. (b) GPR profiles
709 coincident with profiles in (a); the profiles are included after background removal (upper) and
710 overgained. (b), (c) Comparison of anomalies in the different techniques attending the location
711 of magnetic dipoles, homogeneous trends at magnetic field intensity and vertical gradient,
712 hyperbolic anomalies and reflectivity/attenuation changes in the profiles. Conceptual models
713 along 2D sections integrating the geophysical results are also included.

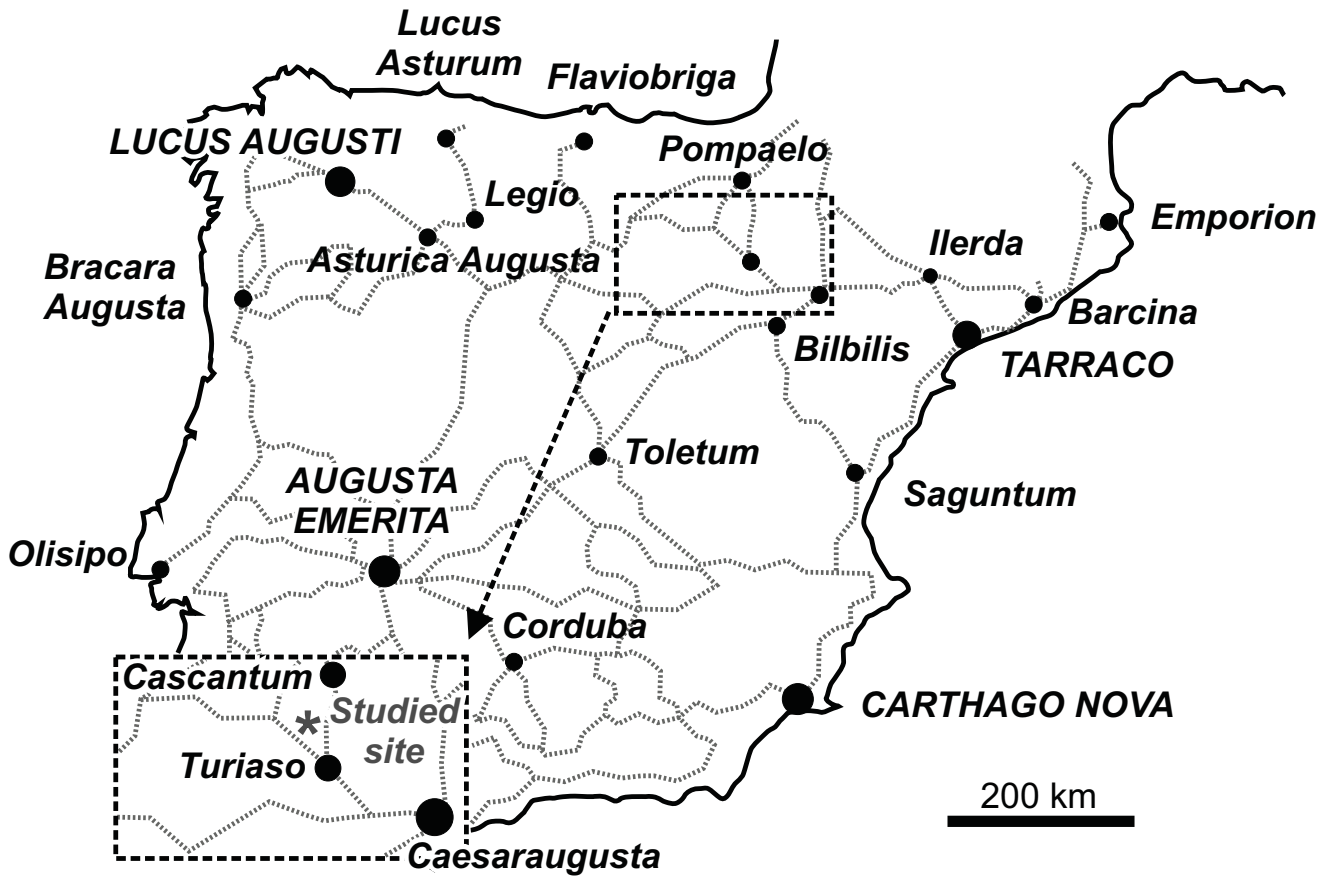
714 Figure 9. Applied methodology in the evaluation of correlation of anomalies obtained from the
715 different geophysical techniques. Conceptual model of interpolation manner; (a) distribution
716 of anomalies, (b) evaluation of lateral correlation of anomalies considering changes in
717 magnetic field and vertical gradient in homogeneous and heterogeneous domains, (c)
718 interpretation of domains and model evaluation of archaeological remains. At (d) an example
719 of integration of GPR data, model construction of anomalies and correlation with changes in
720 Earth's magnetic field and vertical magnetic gradient is included. (e) Distribution of GPR
721 changes along the studied zone that has been used in order to evaluate direct correlation of
722 anomalies by means magnetic data. False relief image of the model obtained from

723 interpolation of anomalies through the integrated analysis exemplified in (a) and following the
724 proposed methodology.

725 Figure 10. (a and b) Photographs of the excavation campaign. (c) Location of sectors excavated
726 in order to constrain the geophysical model. In each of the trenches, a photograph from the
727 excavation and the geophysical model is included. (d) Trench C. (e) Trench D. (f) Trench E.

728 Figure 11. Research phases carried out along the presented study, their interaction and back
729 steps.

Figure 1



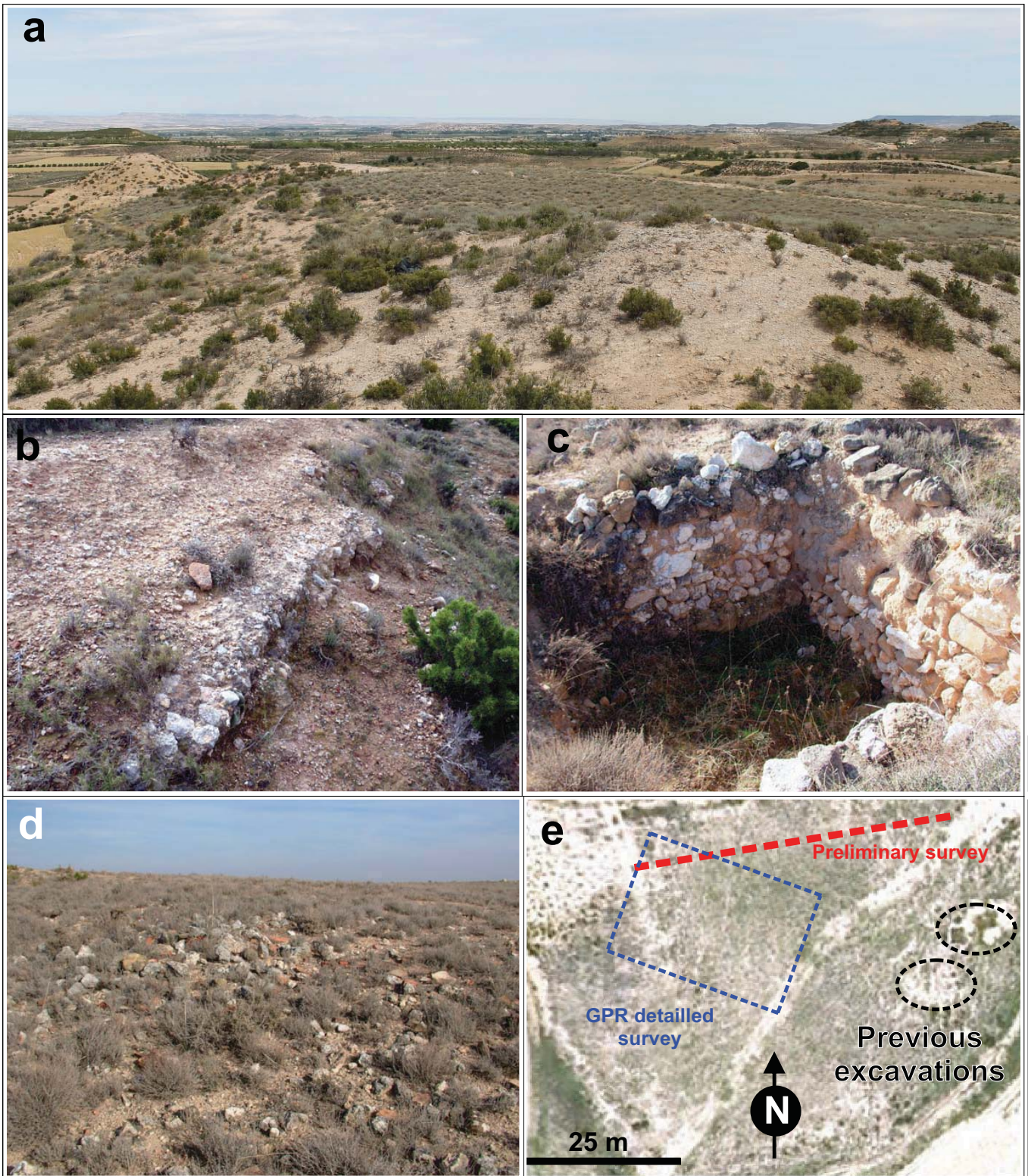


Figure 2

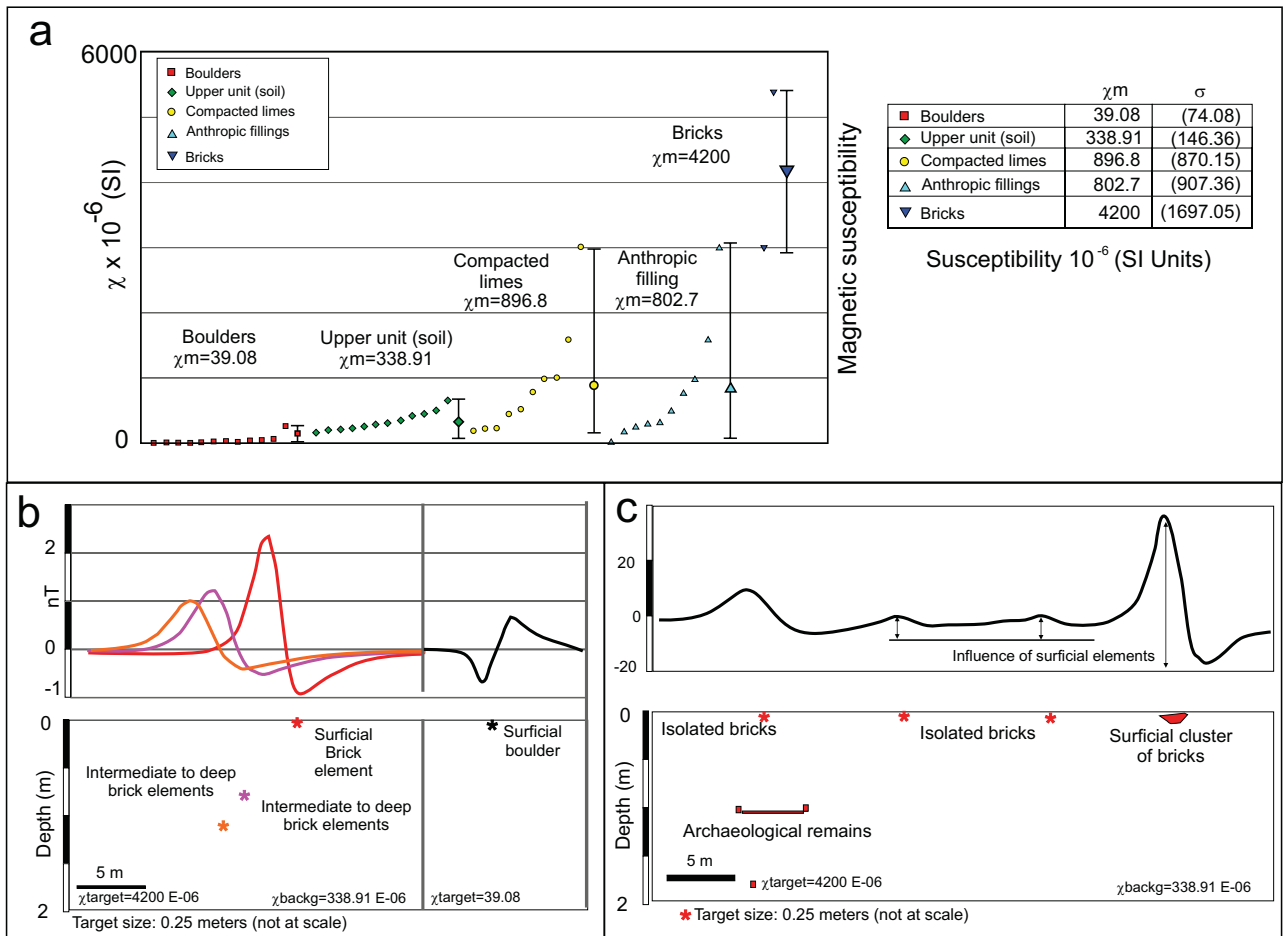


Figure 3

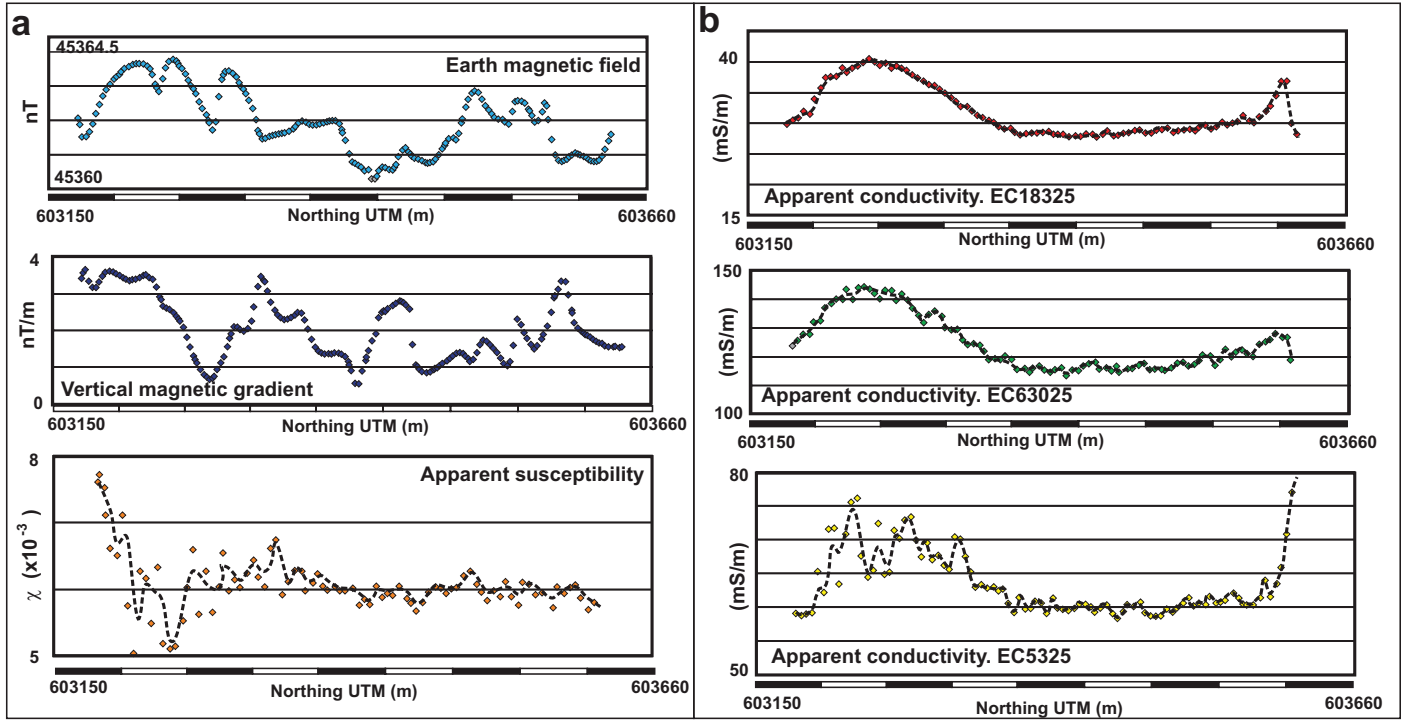


Figure 4.-

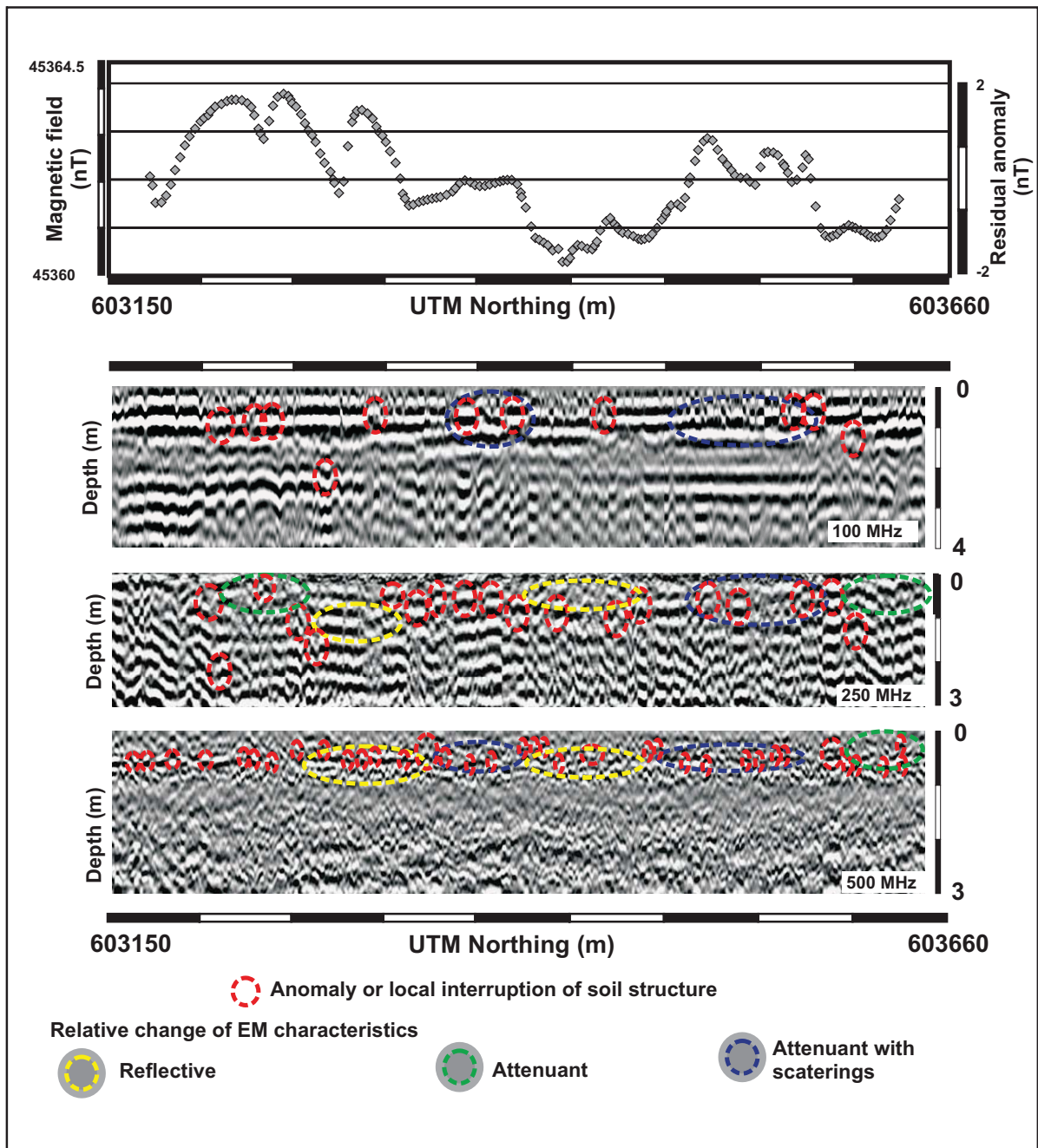


figure 5.-

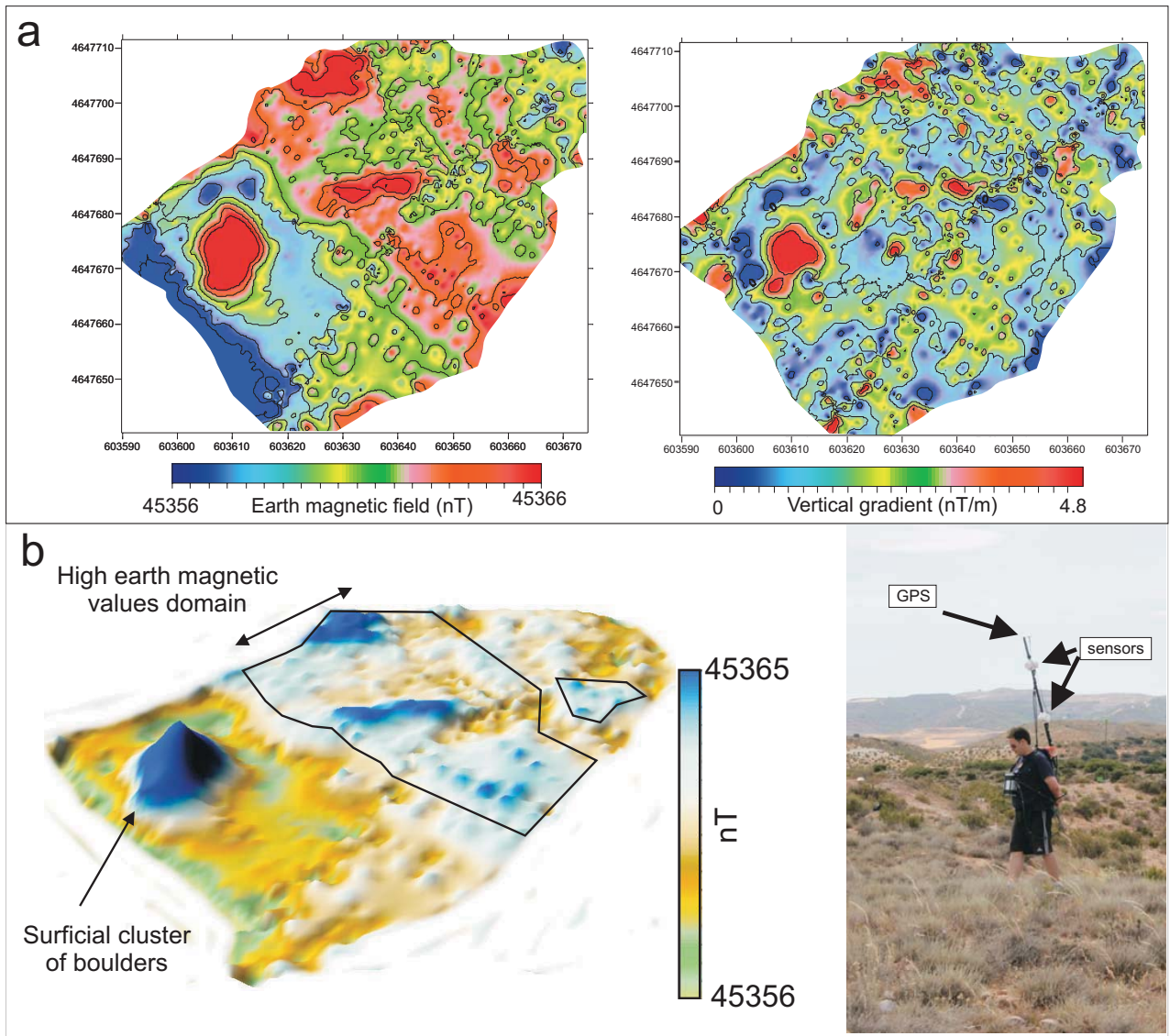


figure 6.-

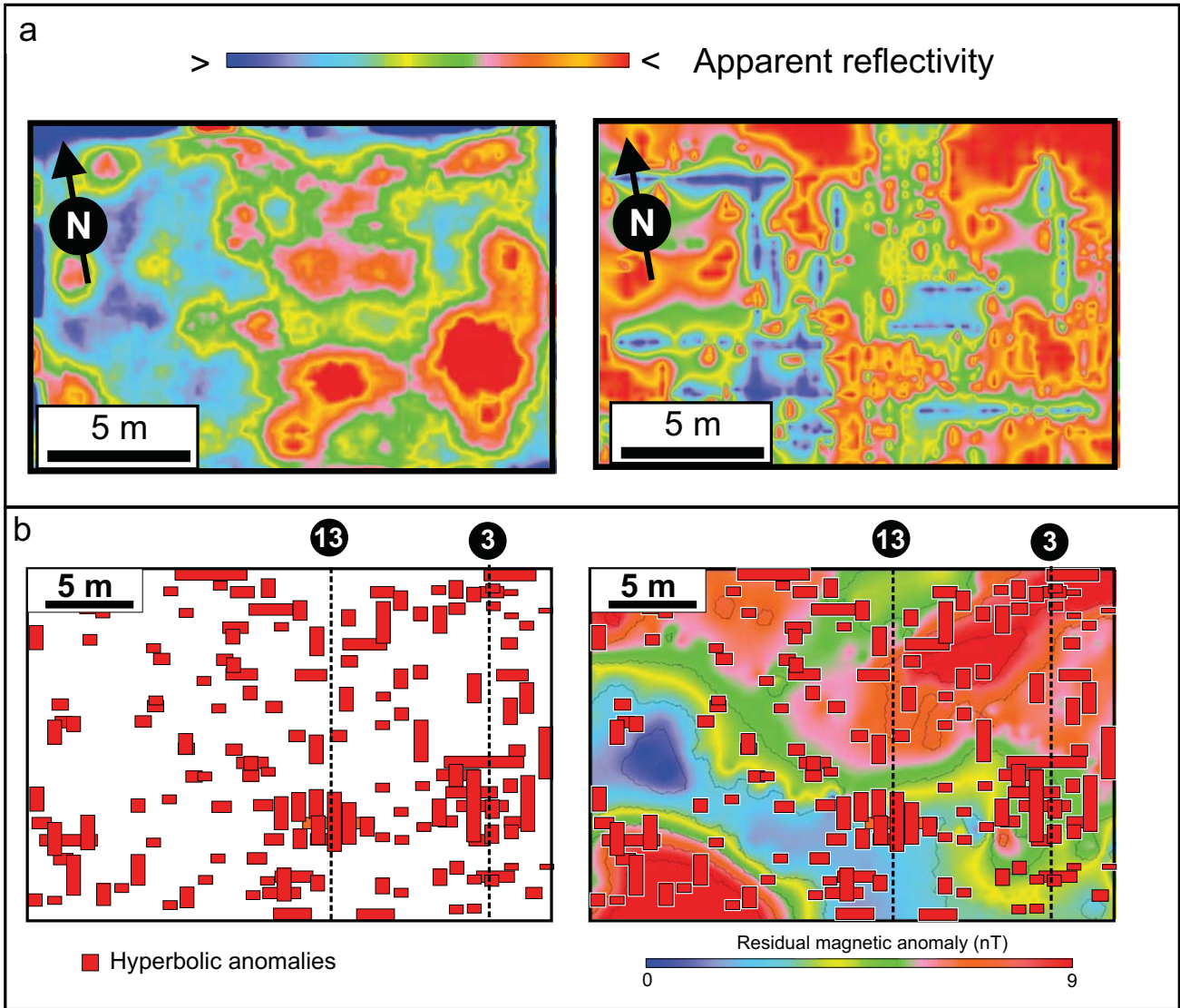


Figure 7

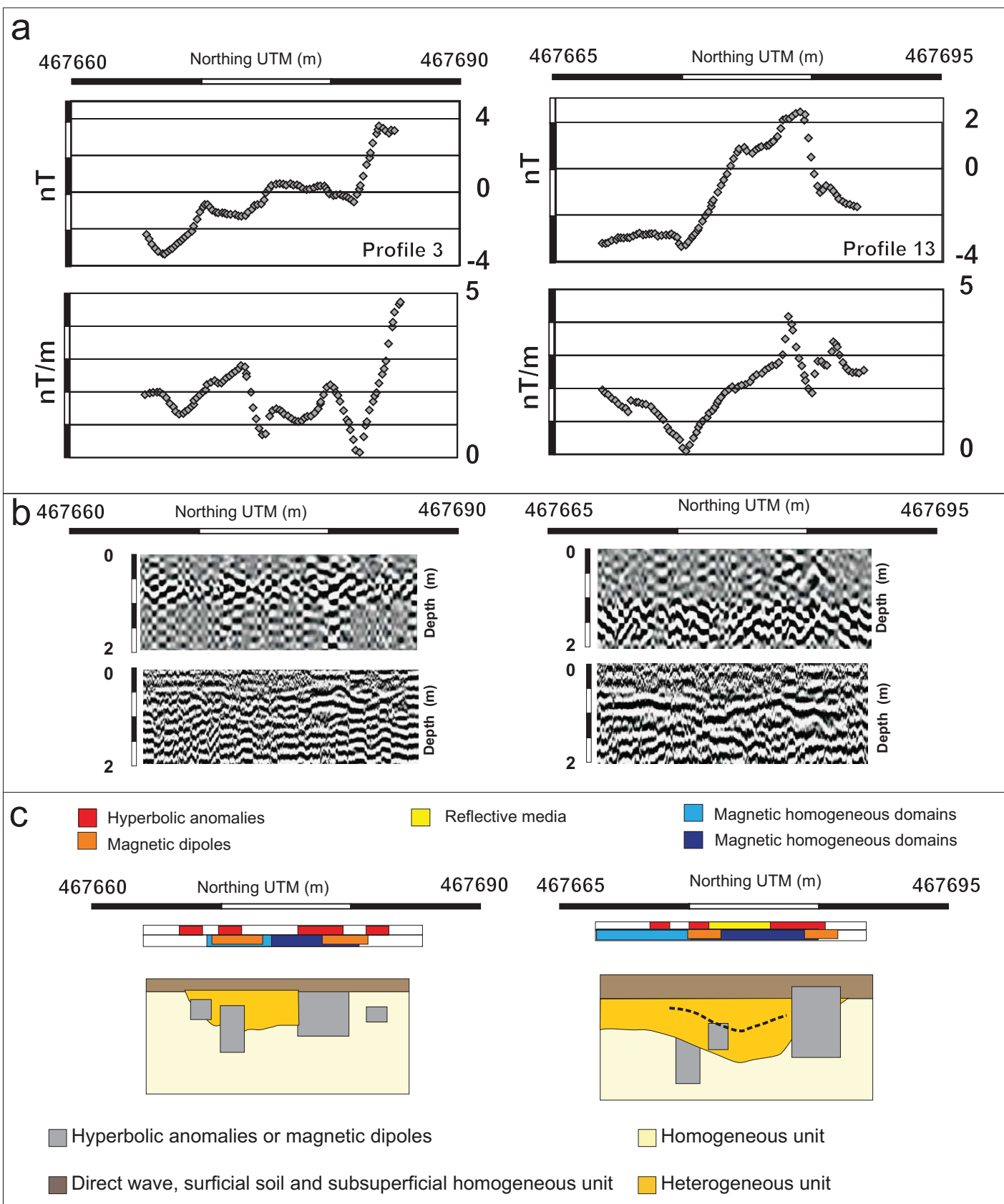


figure 8.-

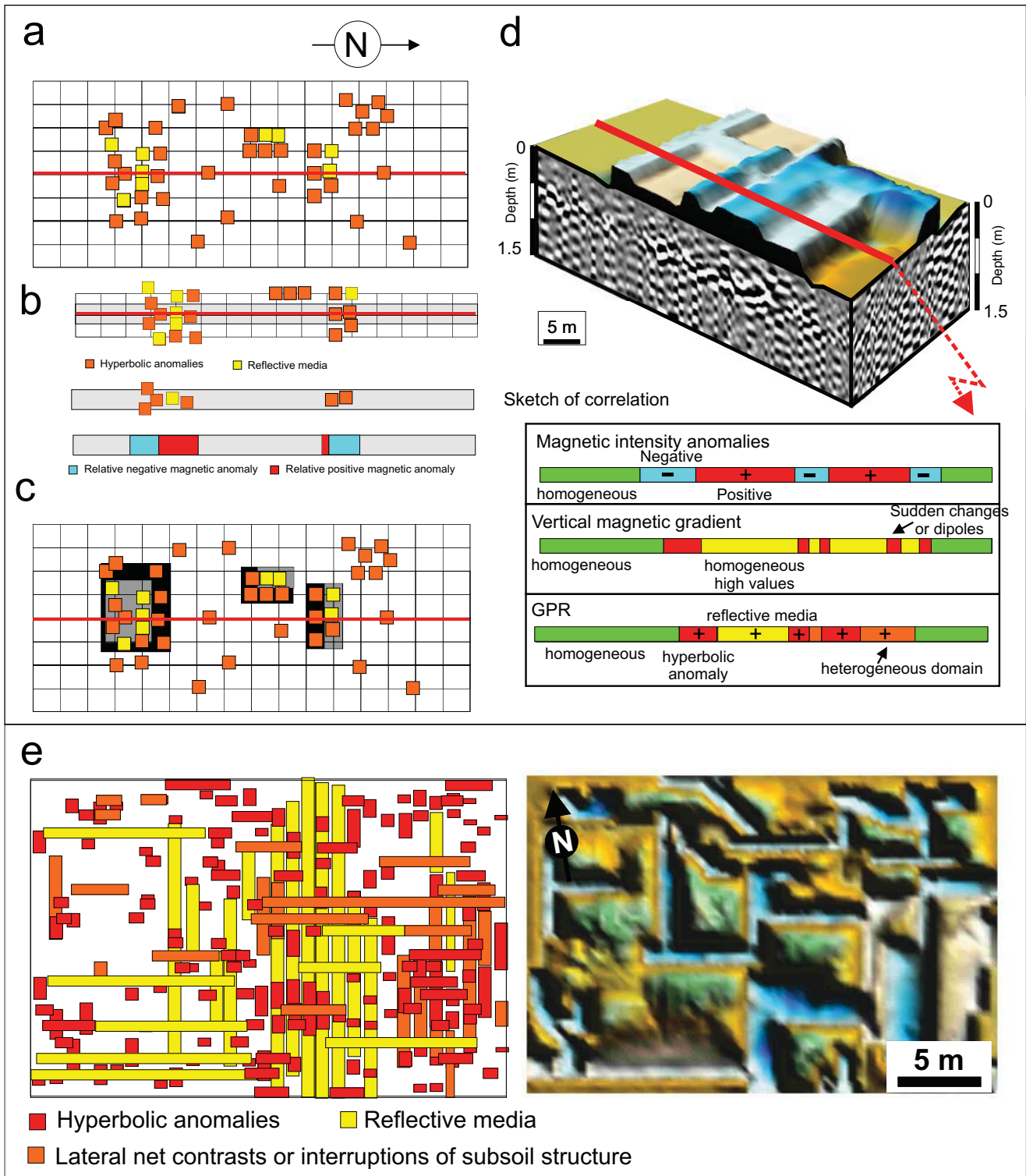


figure 9.-

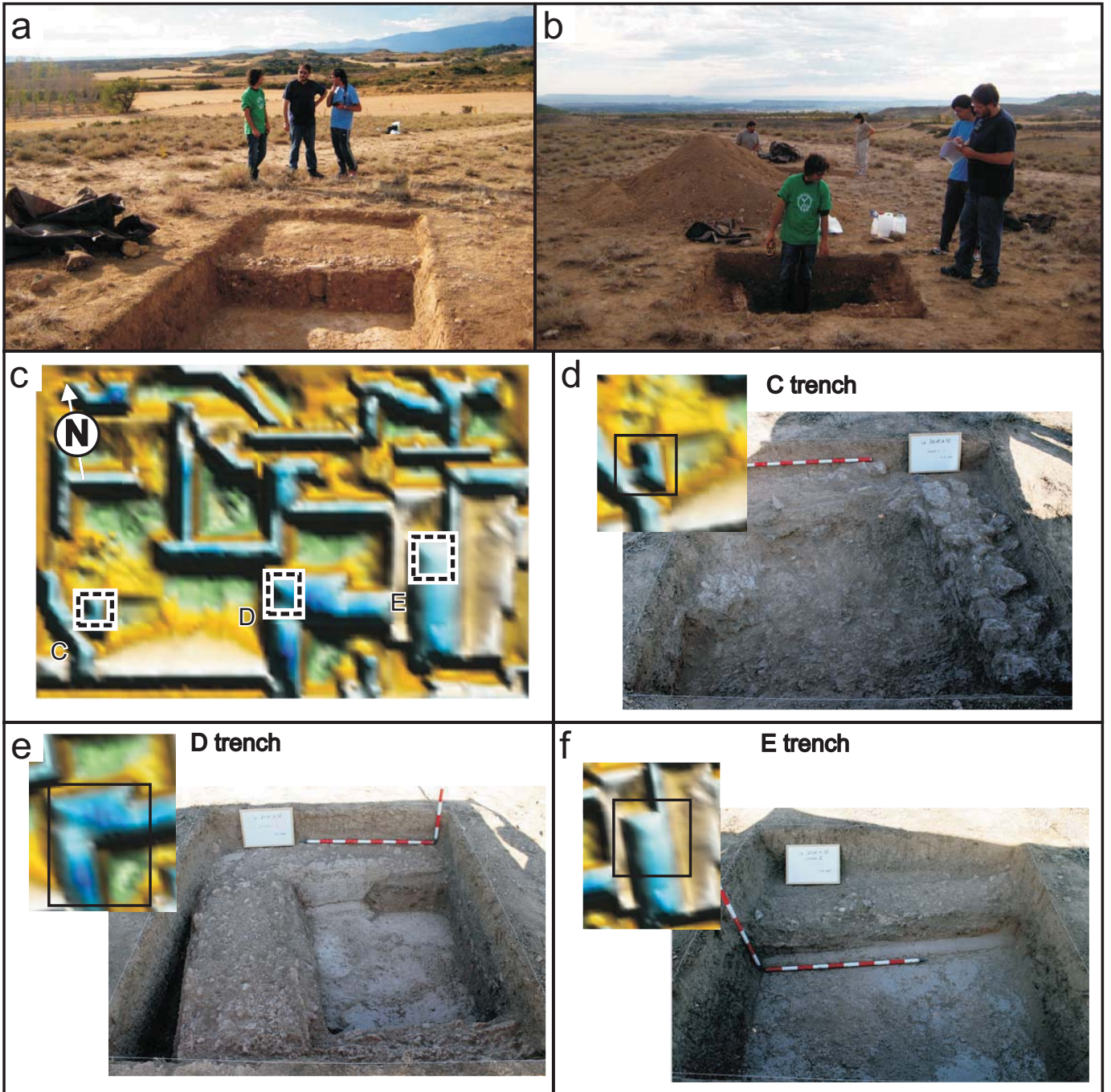


figure 10

